Heliyon 10 (2024) e37307

Contents lists available at ScienceDirect

Heliyon

journal homepage: www.cell.com/heliyon

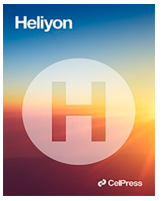

Research article

Quantitative assessment of rotator cuff injuries using synthetic MRI and IDEAL-IQ imaging techniques

Zhaorong Tian, Yabo Ni, Hua He, Bo Tian, Rui Gong, Fenling Xu, Zhijun Wang *

Department of Radiology, General Hospital of Ningxia Medical University, No 804 Shengli Street, Yinchuan, 750001, Ningxia, China

ARTICLE INFO

Keywords:
Rotator cuff injuries
Magnetic resonance imaging
Disease severity
Shoulder pain

ABSTRACT

Purpose: To evaluate synthetic magnetic resonance imaging (SyMRI) and iterative decomposition of water and fat with echo asymmetry and least squares estimation (IDEAL-IQ) imaging for a comprehensive evaluation of rotator cuff injuries (RCI).

Methods: Ninety-seven patients with RCI were classified into four groups based on the arthroscopic results: (grade II), partial tear (grade III), complete tear (grade IV), and controls (grade I). T1 (Transverse Relaxation Time 1), T2 (Transverse Relaxation Time 2), proton density (PD), and fat fraction (FF) were evaluated using SyMRI and IDEAL-IQ. Measurement reliability was assessed using intraclass correlation coefficients (ICC). The diagnostic potential for grading RCI was evaluated using ordinal regression and ROC analyses.

Results: A high measurement reliability (ICC > 0.7) was observed across subregions. T1 and T2 significantly varied across grades, particularly T2 in the lateral subregion between grades III and IV ($P < 0.001$) and the central subregion between grades II and III ($P < 0.001$). ROC analyses yielded valuable diagnostic accuracy, including T2 in the lateral subregion with an AUC of 0.891, distinguishing grade I from grade IV. Positive correlations were found between T2 values in specific shoulder subregions and injury grade ($r = 0.615$ for lateral, $r = 0.542$ for medial, both $P < 0.001$). In grade IV, FF was notably increased in the supraspinatus, infraspinatus, and subscapularis muscles compared with grades I-III. There were no significant FF variations in the teres minor muscle among grades.

Conclusions: Quantitative MRI parameters from SyMRI and IDEAL-IQ, especially T2 and FF, may classify and assess RCI severity. The results could help improve the accuracy of diagnosing different grades of RCI, offering clinicians additional tools for improving patient outcomes through personalized medicine.

1. Introduction

Rotator cuff injuries (RCI) are prevalent and debilitating musculoskeletal disorders causing shoulder pain and restricted mobility, affecting the quality of life of the patients [1–3]. With China's recent economic growth and increased fitness awareness, there has been a notable surge in sports and fitness participation, raising health concerns about sports injuries [4]. A study from West China Hospital of Sichuan University revealed that among 1708 patients with shoulder complaints, RCI was the predominant issue, found in 45.78 % of cases, with 33.33 % being initially misdiagnosed [5]. Globally, there are 200,000 to 300,000 new RCI cases each year, primarily

* Corresponding author.
E-mail address: wangzhijun2056@163.com (Z. Wang).

https://doi.org/10.1016/j.heliyon.2024.e37307
Received 27 March 2024; Received in revised form 26 August 2024; Accepted 30 August 2024
Available online 4 September 2024

Abbreviations

AUC	area under the curve
BMI	body mass index
CI	confidence interval
CT	computed tomography
FF	fat fraction
ICC	intraclass coefficient
IDEAL-IQ	iterative decomposition of water and fat with echo asymmetry and least squares estimation
MAGIC	magnetic resonance image compilation
MRI	magnetic resonance imaging
OR	odds ratio
PD	proton density
PDW	fat-saturated proton density-weighted
RCI	rotator cuff injury
ROC:	receiver operating characteristic
ROI	region of interest
SyMRI	Synthetic magnetic resonance imaging
T1W	T1-weighted
T1	Transverse Relaxation Time (T1)
T1WI FSE	T1-weighted fast spin echo
T2W	T2-weighted
T2	Transverse Relaxation Time (T2)
T2WI FS	fat-saturated T2-weighted imaging
VAS	visual analogue scale

impacting individuals above 50 [5]. Given the high incidence, high misdiagnosis rate, and the aging population globally and in China [6,7], improving the RCI diagnostic accuracy is imperative.

The rotator cuff comprises the supraspinatus, infraspinatus, teres minor, and subscapularis muscles and is vital for the shoulder joint's stability and function [8]. The injuries can range from tendinopathy to partial and complete tears, varying in severity [9–11]. Hence, accurate assessment and grading are crucial for effective treatment decisions in RCI, involving clinical examination and imaging techniques such as ultrasound, magnetic resonance imaging (MRI), and computed tomography (CT) [12]. MRI is highly sensitive for soft tissue injuries and is considered the gold standard for RCI [13]. However, the numerous MRI classifications for preoperative assessment vary in reliability [14], indicating the need for a more objective and precise approach.

T1-weighted (T1W), T2-weighted (T2W), and proton density (PD) sequences are standard MRI sequences for assessing RCI [15]. Synthetic magnetic resonance imaging (SyMRI) is an advanced imaging method that integrates T1W, T2W, and PD that uses post-processing algorithms to create multiple synthetic images and quantitative data, thus improving diagnostic accuracy in numerous diseases [16]. Nevertheless, SyMRI remains under-investigated in musculoskeletal imaging [17], with one study on meniscus injury [18]. In addition, fat infiltration, which can compromise muscle function, may be present in chronic or severe RCI [19]. Iterative decomposition of water and fat with echo asymmetry and least squares estimation (IDEAL-IQ) is an advanced MRI technique that separates and quantifies water and fat signals in the body. IDEAL-IQ was previously used for diagnosing conditions such as cancers [20,21], hemochromatosis [22], and fatty liver disease [23]. It offers quantitative metrics for iron and fat content through proton density fat fraction (FF) [24,25]. Still, the potential of IDEAL-IQ in RCI assessment has yet to be fully explored. Available studies regarding

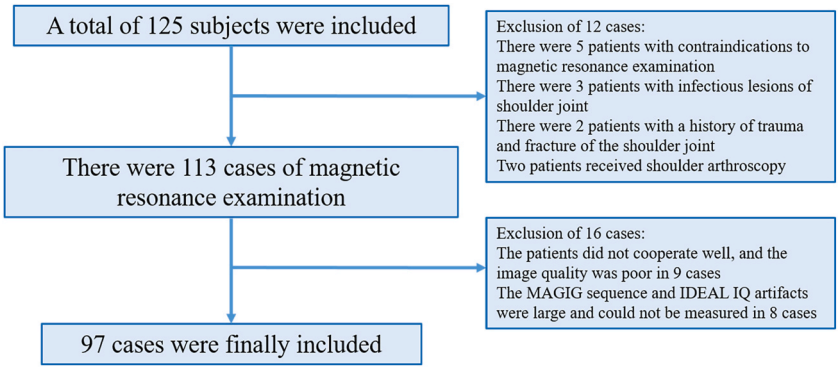

Fig. 1. Flowchart of subject Selection and inclusion Process.

joint imaging were performed for the sacroiliac [26,27] and temporomandibular [28,29] joints.

Therefore, in this study, SyMRI and IDEAL-IQ imaging were used for a comprehensive evaluation of RCI, aiming to assess the efficacy of T1 (Transverse Relaxation Time 1), T2 (Transverse Relaxation Time 2), PD metrics, and FF maps in refining RCI diagnostic accuracy. The results may improve diagnosing and grading RCI accuracy, offering clinicians advanced tools for better patient outcomes.

2. Materials and methods

2.1. Study subjects

A prospective study was conducted at the Orthopedics Outpatient Department of Ningxia Medical University General Hospital (China) from January 2021 to January 2023, enrolling 97 participants who had undergone arthroscopic shoulder surgery. The participants included 54 males and 43 females, aged between 29 and 56 years. RCI was evaluated using arthroscopy. In addition, 28 healthy volunteers, 16 males and 12 females aged between 23 and 49 years with no shoulder abnormalities, were also enrolled. Fig. 1 outlines the key enrollment steps.

The inclusion criteria for the patients were (1) suspected RCI, (2) symptoms for 1–24 months, (3) age between 18 and 60 years, (4) no previous standardized treatment, and (5) no previous shoulder joint surgery.

For the control group, the inclusion criteria were (1) age between 18 and 60 years, (2) no abnormal lesions on routine MRI scans of the shoulder, (3) no MRI contraindications, and (4) no history of trauma, surgery, tumors, or inflammatory conditions.

The exclusion criteria for all participants were (1) confirmed infectious lesions, fractures, or space-occupying shoulder lesions as detected by MRI or X-ray, (2) presence of rheumatic diseases, such as rheumatoid arthritis, joint tuberculosis, or neuropathic joint diseases, or (3) MRI contraindications, such as internal cardiac metallic valves, neural stimulators, cardiac pacemakers, arterial clips, inner ear implants, intraocular metallic foreign bodies, metal prostheses, or ferromagnetic foreign bodies.

According to the inclusion and exclusion criteria, the participants in the control group were classified as grade I (no pathological symptoms of the rotator cuff, the morphology of the supraspinatus tendon in MRI images was normal and continuous, and each sequence showed uniform and consistent low intensity). According to the results of shoulder arthroscopy and Zlatkin grading criteria, the participants with RCI were divided into three groups: grade II (tendinopathy group; rotator cuff contusion and pathological manifestations of tendon congestion, edema and even fibrosis, reducible injury), grade III (partial tear group; incomplete laceration injury and rotator cuff injury resulting in partial tear of rotator cuff tendon fibers, which can occur on the articular surface of the supraspinatus tendon or the side of the capsule and inside the tendon), and grade IV (complete tear group; full-thickness tendon rupture that results in penetrating injury to the inferior acromial bursa and glenohumeral joint, resulting in a complete tear).

2.2. Assessment of RCI

The duration of symptoms was recorded. Pain severity was assessed using the Visual Analog Scale (VAS). The VAS categories were defined as 0 = no pain, 1–3 = mild pain, 4–6 = moderate pain, and 7–10 = severe pain [30].

2.3. MRI

MRI of the shoulder joint was conducted using a SIGNA™ Architect 3.0-T scanner (GE, USA) with a dedicated 16-channel shoulder coil. The patients were positioned supine with their hands naturally at their sides. Sandbags were used to stabilize the shoulder and minimize motion artifacts. Scans were centered on the humeral head, covering the clavicular acromion to the upper humerus. The imaging protocol included axial T1-weighted fast spin echo (T1WI FSE), axial fat-saturated T2-weighted imaging (T2WI FS), oblique coronal T2WI FS, and oblique sagittal fat-saturated proton density-weighted (PDW) sequences. It was followed by oblique coronal magnetic resonance image compilation (MAGIC, GE-proprietary sequences) sequences and oblique sagittal least squares estimation with asymmetric echo IDEAL-IQ. The MRI sequences and parameters for shoulder joint imaging are shown in Table S1.

2.4. Post-processing of MAGIC sequence images

SyMRI and IDEAL-IQ are advanced MRI techniques that use post-processing algorithms to create images with synthetic contrasts. As for classical MRI, synthetic T1WI, T2WI, and PDW images can be generated. IDEAL-IQ also generates the FF parameter. After the MAGIC sequence scan, image post-processing and data recording for T1W, T2W, and PD mapping were done using the MAGIC software (GE). For the T2WI FS oblique coronal images, a segmentation method [31] was used to divide the supraspinatus tendon into three subregions: lateral, central, and medial (Fig. S1). The lateral subregion referred to the distal insertion area of the supraspinatus tendon fibers. The central subregion represented the midpoint between the lateral and medial areas. The medial subregion was approximately 2 cm inward from the lateral area, just above the humeral head cartilage. In cases of complete supraspinatus tendon tears, measurements were taken from the three subregions of the retracted tendon portion. Regions of interest (ROIs) were individually positioned within the three subregions while avoiding surrounding fat, fluid, and other soft tissues. Efforts were made to ensure ROI alignment with the contour of the tendon, and T1, T2 and PD values were measured for each subregion. Of note, some patients with grade IV injuries could not be included because the supraspinatus tendon was completely torn and, in some cases, had severe retraction of the severed end. Therefore, their T2 value could not be measured due to the influence of surrounding effusion.

2.5. Post-processing of IDEAL-IQ sequence images

After the IDEAL-IQ sequence scan, FF images were transferred to the ADW 4.7 post-processing workstation (GE). Following the methodology from a previous study [32], the research plane was selected based on the presence of a shaped scapular structure. ROIs were delineated on the FF images to outline the supraspinatus, infraspinatus, subscapularis, and teres minor muscles. Emphasis was made to follow the outer muscle contours while avoiding adjacent tissues. The FF value was determined for each muscle.

2.6. Data quality control

All participants underwent MRI scans for routine sequences as well as oblique coronal MAGIC sequences and oblique sagittal IDEAL-IQ sequences to ensure data quality. Two experienced radiologists in musculoskeletal diseases (observers 1 and 2) independently performed ROI delineation and data recording. These measurements were repeated with a 2-week interval to assess interobserver and intraobserver consistency. The final dataset represented an average of the four readings.

2.7. Grading of RCI

The control group, designated as grade I [33], consisted of symptom-free volunteers with MRI-confirmed normal supraspinatus tendon morphology. The patient group was categorized based on shoulder arthroscopy and the Zlatkin grading system [34,35] into three grades: grade II (tendonopathy group) included patients with reversible shoulder cuff injuries, presenting tendon congestion, edema, or fibrosis; grade III (partial tear group) comprised those with partial supraspinatus tendon tears, either on the joint surface or within the tendon; and grade IV (complete tear group) involved patients with full-thickness tendon ruptures extending into the glenohumeral joint. Two experienced surgical specialists and a musculoskeletal radiologist with over a decade of expertise independently graded the injuries blindly. In grading, differences arose, and consensus was achieved through collaborative discussion.

2.8. Statistical analysis

Statistical analysis was performed using SPSS 26.0, MedCalc 19.0, and GraphPad Prism 8.0 software. The normality of the quantitative variables was assessed through the Kolmogorov-Smirnov test. Normally distributed values were expressed as mean ± standard deviation and were compared using a one-way analysis of variance. Non-normally distributed data were presented as median (interquartile range) and analyzed using non-parametric tests. Categorical data were represented as percentages (%) and compared using the chi-squared test. Spearman's correlation analysis was used to assess the relationships between various parameters. Reproducibility was evaluated using the interclass correlation coefficient (ICC), where ICC values less than 0.5 indicated poor consistency, values between 0.5 and 0.7 signified moderate consistency and values exceeding 0.7 indicated good consistency. The data for ICC come from the same measurement location for each patient. Logistic regression analysis was performed to identify predictors for RCI grades. Receiver operating characteristic (ROC) curves were constructed for these parameters, and their diagnostic performance was evaluated based on sensitivity, specificity, 95 % confidence intervals (CI), Youden's index, and area under the curve (AUC). AUC comparisons were conducted using the Z-test. Friedman's test was used to compare average FF values. A P-value less than 0.05 was considered statistically significant.

3. Results

3.1. Comparative analysis of RCI grades

A total of 125 patients were enrolled, but 12 were excluded due to contraindications to MRI (n = 5), infection lesions in the shoulder joint (n = 3), history of trauma and shoulder fracture (n = 2), and arthroscopy (n = 2). Then, 113 patients underwent MRI, but 16 were

Table 1
Comparison of clinical characteristics between patients and healthy controls.

	Patients (n = 97)	Healthy controls (n = 28)	t/X^2	P
Age (years)	37 ± 6.44	35 ± 5.98	0.32	0.71
Sex, n (%)				
Male	54 (55.7)	16 (57.1)	8.00	0.24
Female	43 (44.3)	12 (42.9)		
BMI/(kg·m^{-2})	20.84 ± 1.57	21.09 ± 1.64	0.24	0.69
Laterality, n (%)				
Left	47 (48.4)	14 (50)	4.00	0.26
Right	50 (51.6)	14 (50)		
Grade, n (%)				
I		28 (22.4)		
II	37 (29.6)			
III	34 (27.2)			
IV	26 (20.8)			

excluded because of poor patient cooperation and image quality (n = 9) and MAGIC or IDEAL-IQ artifacts (n = 8). Therefore, 97 patients with RCI were included in the study, including 37 with grade II, 34 with grade III, and 26 with grade IV. The control group (grade I) consisted of 28 individuals. There were no statistically significant differences in age, sex, laterality, and body mass index between the patient and the control groups (all $P > 0.05$; Table 1).

3.2. Consistency of measurements

As shown in Table 2, all T1, T2 and PD measurements showed strong intraobserver and interobserver agreement, with ICC values consistently greater than 0.7 across the lateral, central, and medial subregions. The FF measurements also exhibited high consistency between and within the two observers, with all ICC values greater than 0.75 (Table 3). The results underscore the reliability of these measurements in clinical practice.

3.3. Analysis of T1, T2 and PD values across RCI grades

As shown in Fig. 2 (and Supplementary Table S2), the T1 values in the lateral subregion displayed a significant difference across the four grades ($P < 0.001$). In contrast, the T1 values in the central and medial subregions showed no significant differences across the grades ($F = 1.507$ and 1.933, $P = 0.216$ and 0.128, respectively) (Fig. 2A). For the T2 values, significant differences were observed in the lateral subregion between grades III and IV and in the central subregion between grades II and III (both $P < 0.001$). However, the medial subregion's T2 values did not significantly vary across the grades ($F = 3.654$, $P = 0.014$) (Fig. 2B). As for the PD values, no subregions demonstrated significant differences across the grades ($F = 5.377$, 2.618, and 1.349, $P = 0.012$, 0.054, and 0.261, respectively) (Fig. 2C). The data suggests that a deeper analysis of T2 could be beneficial, particularly for the lateral and central subregions.

3.4. T2 measurements in lateral and central subregions can differentiate between grades of RCI

Ordinal regression analysis demonstrated that the T2 values in the lateral and central subregions exhibited statistically significant differences across grades ($P < 0.001$). Specifically, the regression coefficients were 0.1160 and 0.1146, with corresponding odds ratios (OR) of 1.123 (95 % CI: 1.037–1.216) and 0.122 (95 % CI: 1.151–1.197), respectively.

In the ROC curve analysis (Table 4), the T2 values in the lateral subregion yielded AUCs of 0.891, 0.797, and 0.723 for distinguishing between grade I and grade IV, grade II and grade IV, and grade III and grade IV, respectively. For the central subregion, the AUCs for T2 values were 0.946, 0.886, and 0.746 for the same classifications (Fig. 3A–D). In addition, the AUC for the T2 values in differentiating grade I from grade III was 0.843 (Fig. 3E). When comparing the diagnostic capacities of T2 values in the lateral and central subregions, a Z-test showed no statistically significant difference between their AUCs for discerning grade I from grade IV and grade II from grade IV ($Z = 1.097$ and 1.261, $P = 0.275$ and 0.216, respectively). These results highlight the diagnostic accuracy of T2 measurements in assessing various RCI grades.

3.5. T2 values in lateral and medial shoulder subregions correlate with RCI grading

T2 values of the lateral and medial subregions positively correlated with the grading of the injuries ($r = 0.615$ for lateral and 0.542 for medial, respectively; both $P < 0.001$; Fig. 4). It suggests a specific association of T2 values in certain subregions with injury grading. We evaluated different levels of rotator cuff injuries through shoulder MRI imaging. First, T2WI FS images and integrated MRI pseudocolor images exhibited different characteristics at each injury level: The T2WI FS images in the normal group showed clear and uniform rotator cuff structures with no obvious signal abnormalities (Fig. 5 1A-D). The pseudocolor images also displayed uniform tissue contrast with no abnormal signal distribution. In the tendinopathy group, T2WI FS images showed slightly increased signal intensity in the rotator cuff area, indicating early degeneration of the tendon tissue. The pseudocolor images further displayed slight signal enhancement in the T2 mapping images, reflecting changes in the microstructure of the tissue(Fig. 5 2A-D). In the partial tendon tear group, the T2WI FS images showed a notably high-signal area, suggesting edema or inflammatory response in the partially torn region. The pseudocolor images displayed significant signal enhancement, indicating substantial pathological changes in the torn tissue. In the full-thickness tendon tear group, the high-signal area in the T2WI FS images further expanded, showing extensive tendon rupture and surrounding tissue lesions (Fig. 5 3A-D). The pseudocolor images revealed obvious abnormal signal areas, particularly in the T2 mapping images, where the torn area showed significant signal enhancement, indicating increased severity of edema and

Table 2
ICC Values of T1, T2, and PD measurements by observers.

	T1 value			T2 value			PD value		
	Lateral	Central	Medial	Lateral	Central	Medial	Lateral	Central	Medial
Observer 1	0.905	0.847	0.885	0.909	0.824	0.827	0.922	0.915	0.795
Observer 2	0.917	0.909	0.896	0.912	0.916	0.809	0.876	0.879	0.723
Interobserver	0.911	0.899	0.917	0.911	0.906	0.879	0.933	0.901	0.755

The data come from the same measurement location for each patient.

Table 3
ICC values of fat fraction measurements in shoulder rotator cuff muscles by observers.

	Fat fraction			
	Supraspinatus muscle	Infraspinatus muscle	Subscapularis muscle	Teres minor muscle
Observer 1	0.901	0.896	0.904	0.912
Observer 2	0.903	0.892	0.877	0.933
Interobserver	0.910	0.903	0.897	0.876

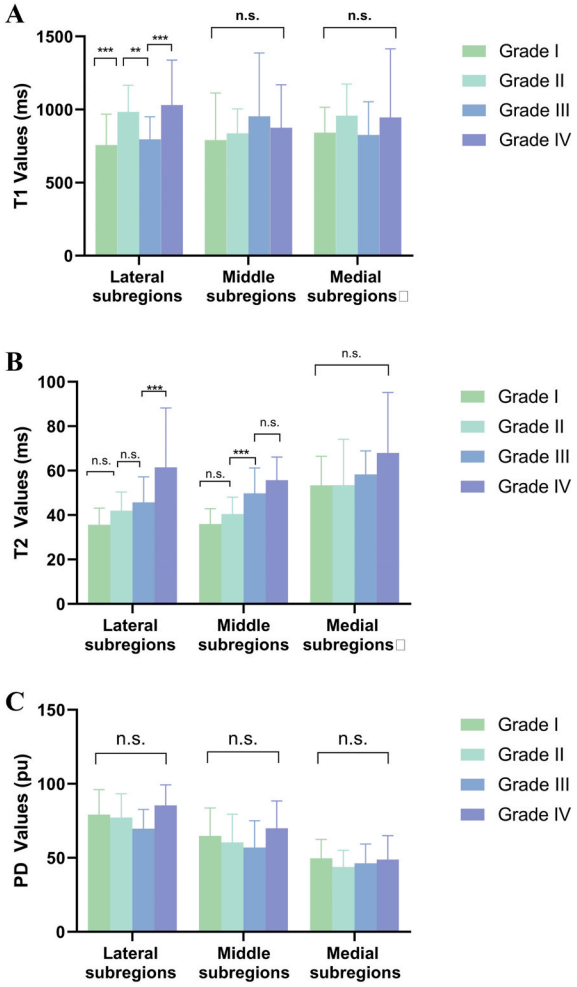

Fig. 2. Comparison of T1 (A), T2 (B) and PD (C) values corresponding to different grades of RCI in the lateral, central, and medial subregions of the supraspinatus muscle tendon. Data are expressed as mean ± standard deviation (SD). **P < 0.01, ***P < 0.001, n.s, no statistically significant difference.

fibrosis. As the severity of rotator cuff injury increased, the abnormal signal intensity and distribution in T2WI FS images and pseudocolor images gradually worsened, reflecting the pathological progression of the rotator cuff from normal to degeneration to tear (Fig. 5 4A-D).

3.6. FF values indicate RCI severity

The FF values for the supraspinatus, infraspinatus, and subscapularis muscles in grade IV injuries were significantly elevated compared with the other grades (all P < 0.001). However, the teres minor muscle showed no significant variations across different groups (Z = 5.760, P = 0.259; Fig. 6A). MRI images of the shoulder joint comparing grade I (upper) to grade IV (lower) are shown in Fig. 6B.

Furthermore, Spearman correlation analysis revealed positive correlations between the FF values of the supraspinatus and

Table 4
ROC curve analysis using T2 values from the lateral and middle subregions for diagnosing different grades of RCI.

Grading		Sensitivity	Specificity	Youden's Index	AUC (95%CI)	P
Lateral subregion T2 value	Grade I vs. Grade II	0.636	0.786	0.520	0.750(0.626–0.874)	0.053
	Grade II vs. Grade III	0.735	0.706	0.356	0.721(0.598–0.884)	0.049
	Grade III vs. Grade IV	0.885	0.471	0.356	0.723 (0.594–0.853)	<0.001
	Grade I vs. Grade IV	0.885	0.821	0.706	0.891 (0.801–0.981)	<0.001
	Grade II vs. Grade IV	0.538	0.976	0.514	0.797 (0.680–0.914)	<0.001
Middle subregion T2 value	Grade I vs. Grade II	0.362	0.790	0.493	0.636(0.493–0.778)	0.056
	Grade II vs. Grade III	0.735	0.786	0.521	0.746 (0.631–0.861)	<0.001
	Grade III vs. Grade IV	0.265	1.000	0.265	0.636(0.495–0.777)	0.072
	Grade I vs. Grade III	0.735	0.893	0.628	0.843 (0.745–0.941)	<0.001
	Grade I vs. Grade IV	0.962	0.821	0.783	0.946 (0.849–0.989)	<0.001
	Grade II vs. Grade IV	0.923	0.738	0.661	0.886 (0.809–0.962)	<0.001

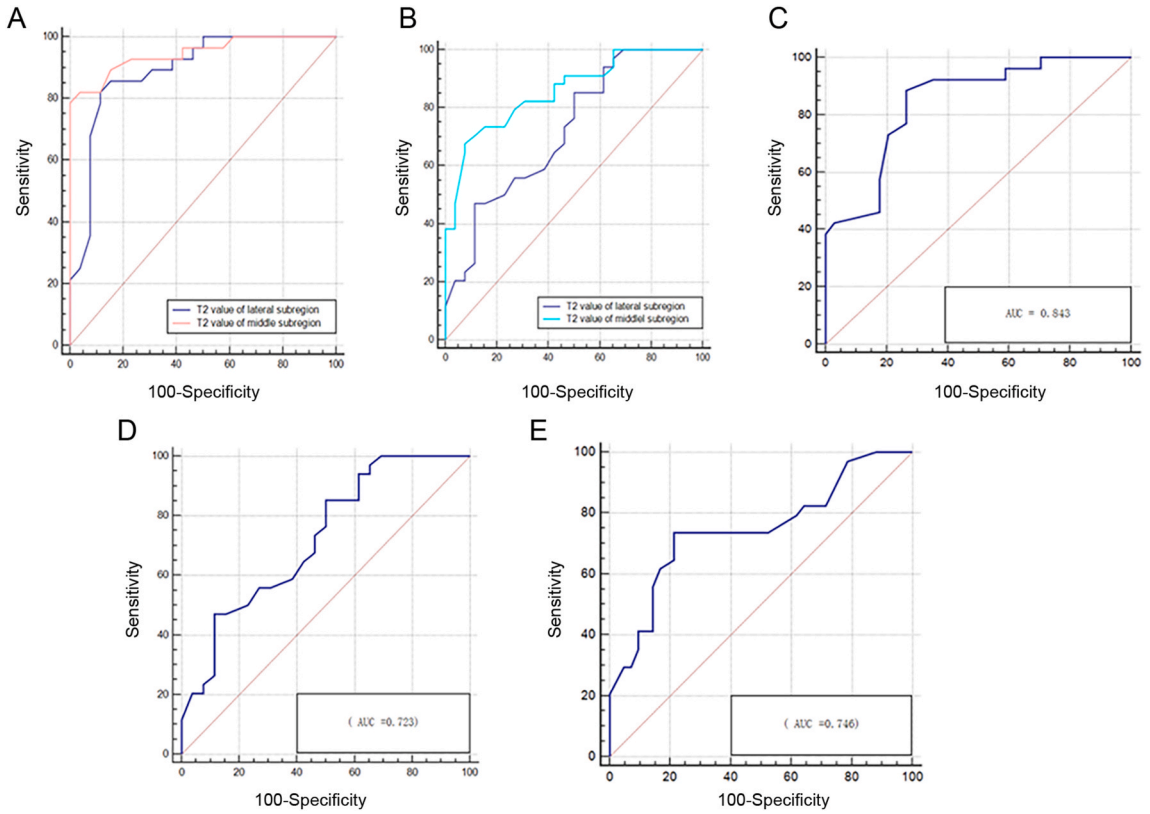

Fig. 3. Evaluation of T2 values in lateral and medial subregions for grading rotator cuff injuries (RCI). (A, B) Receiver operating characteristic (ROC) curve for the diagnosis of grade II vs. grade IV (A) and grade I vs. grade IV (B) using T2 values from the lateral and medial subregions. (C) ROC curve for the diagnosis of grade II vs. grade III RCI using T2 values from the medial subregion. (D) ROC curve for the diagnosis of grade III vs. grade IV RCI using T2 values from the lateral subregion. (E) ROC curve for the diagnosis of grade I vs. grade III RCI using T2 values from the medial subregion.

infraspinatus muscles and RCI grading ($r = 0.715$ and 0.628, respectively, both $P < 0.001$). Conversely, the teres minor and subscapularis muscles showed no notable correlation in FF values with injury grading ($P > 0.001$). No significant associations existed between the FF values of the supraspinatus, infraspinatus, teres minor, and subscapularis muscles and VAS scores (all $P > 0.001$). However, a positive correlation was established between symptom duration and the FF values for the supraspinatus ($r = 0.710$, $P < 0.001$), infraspinatus ($r = 0.587$, $P < 0.001$), and subscapularis muscles ($r = 0.379$, $P < 0.001$). At the same time, the teres minor displayed a weak yet significant correlation ($r = 0.306$, $P = 0.004$). These results suggest that the FF values can serve as indicators of RCI severity, except in the teres minor muscle.

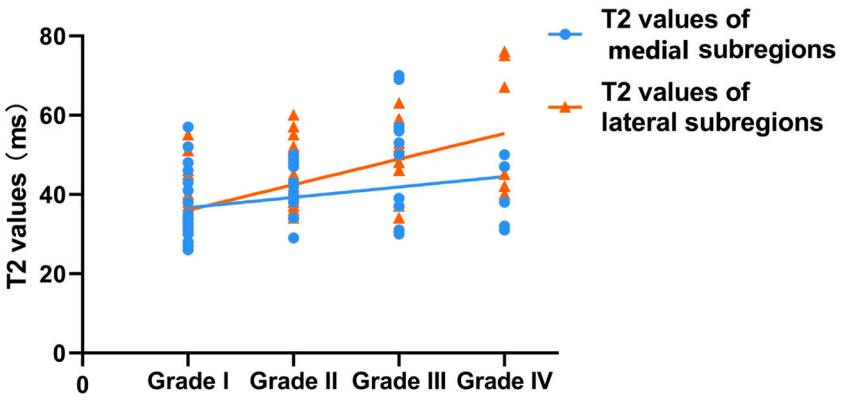

Fig. 4. A Spearman correlation analysis was conducted to examine the relationship between T2 values in the lateral and medial subregions and the grading of RCI.

3.7. Correlations between FF values and clinical parameters

The FF values in the supraspinatus ($r = 0.240$, $P = 0.042$) and infraspinatus ($r = 0.273$, $P = 0.020$) muscles were correlated with symptom duration (Supplementary Table S3 and Supplementary Fig. S2A). The FF values in the supraspinatus ($r = 0.364$, $P = 0.003$), infraspinatus ($r = 0.313$, $P = 0.007$), and teres minor ($r = 0.349$, $P = 0.003$) muscles were correlated with age (Supplementary Table S4 and Supplementary Fig. S2B).

4. Discussion

In this study, 97 patients with RCI were graded based on the arthroscopic findings. The results suggest that the T2 values in the lateral and central shoulder subregions had a strong differentiating power among various RCI grades, as indicated by significant correlations and high diagnostic accuracy. In addition, the FF values proved reliable indicators of RCI severity, particularly in the supraspinatus, infraspinatus, and subscapularis muscles. These imaging biomarkers may enhance the clinical evaluation and treatment planning for patients with RCI.

Deep learning techniques based on MRI and ultrasound images are being investigated but are not mature yet [33,36]. Other methods are based on classical MRI images but are limited by the precision of the images [37–40]. When evaluating the consistency of quantitative measurements in SyMRI, strong interobserver and intraobserver ICC values were observed for the three subregions of the supraspinatus tendon, with the highest consistency generally found in the lateral subregion, consistent with previous research findings [41]. The prominence of the lateral subregion's attachment to the greater tuberosity of the humerus allows for clear and distinct delineation, leading to enhanced consistency in quantitative measurements among observers. The ICC value for the central subregion ranked second highest. Tendon continuity in the shoulder joint images affects measurements in this subregion. Deviations in scan positioning or improper patient placement may cause positional displacement during region delineation, impacting measurement stability. Regarding the inner subregion, it transitions into muscle as tissue composition changes. During ROI outlining, the observer's subjective judgment can influence ROI placement, causing slight deviations. It may modestly reduce the consistency in quantitative measurements for the inner subregion. However, overall, the quantitative measurements of all three subregions exhibit relatively high consistency, indicating their potential clinical applicability.

When assessing RCI, the T1 values in the lateral subregion were significantly different across grades. In contrast, T2 values in the lateral subregion varied between grades III and IV and in the central subregion between grades II and III. However, PD values showed no significant differences across subregions or grades. Notably, as the severity of RCI increased, the T2 values of the supraspinatus muscle tendon gradually rose, while T1 and PD values did not show a corresponding trend. In grade IV injuries, T2 values significantly increased in the lateral subregion compared with the other grades. Similarly, T2 values were significantly higher in the central subregion than in grades I and II. From an anatomical perspective, the portion of the supraspinatus muscle tendon attaching to the greater tubercle of the humerus, known as the lateral subregion, has a limited blood supply. In RCI, this region is termed the "hypovascular zone" [42] and is prone to ischemic edema, resulting in increased water content and longer T2 relaxation times on MRI images. In addition, since collagen and fibrous protein molecules are major components of tendons, any disruption of these components due to inflammation, partial tears, complete tendon rupture, and edema at the ruptured tendon ends contribute to a significant increase in T2 values. This observation aligns with previous research [43]. On the other hand, T1 values are valuable for diagnosing fat infiltration, fibrosis, and tissue edema. However, tendon degeneration primarily involves changes in water content and collagen fibers, making T2 values more sensitive to tissue edema [44,45]. Consequently, T1 values do not significantly vary among different grades. As for PD values, representing hydrogen protons in tissues, they have not been extensively studied in musculoskeletal diseases, particularly in tendons. Meanwhile, theoretically, proton content in tendons might change during injury. This study did not find a link between PD values and the grading of RCI. Further animal-based research is needed.

In this study, T2 values in the lateral and central subregions demonstrated significant diagnostic potential for differentiating

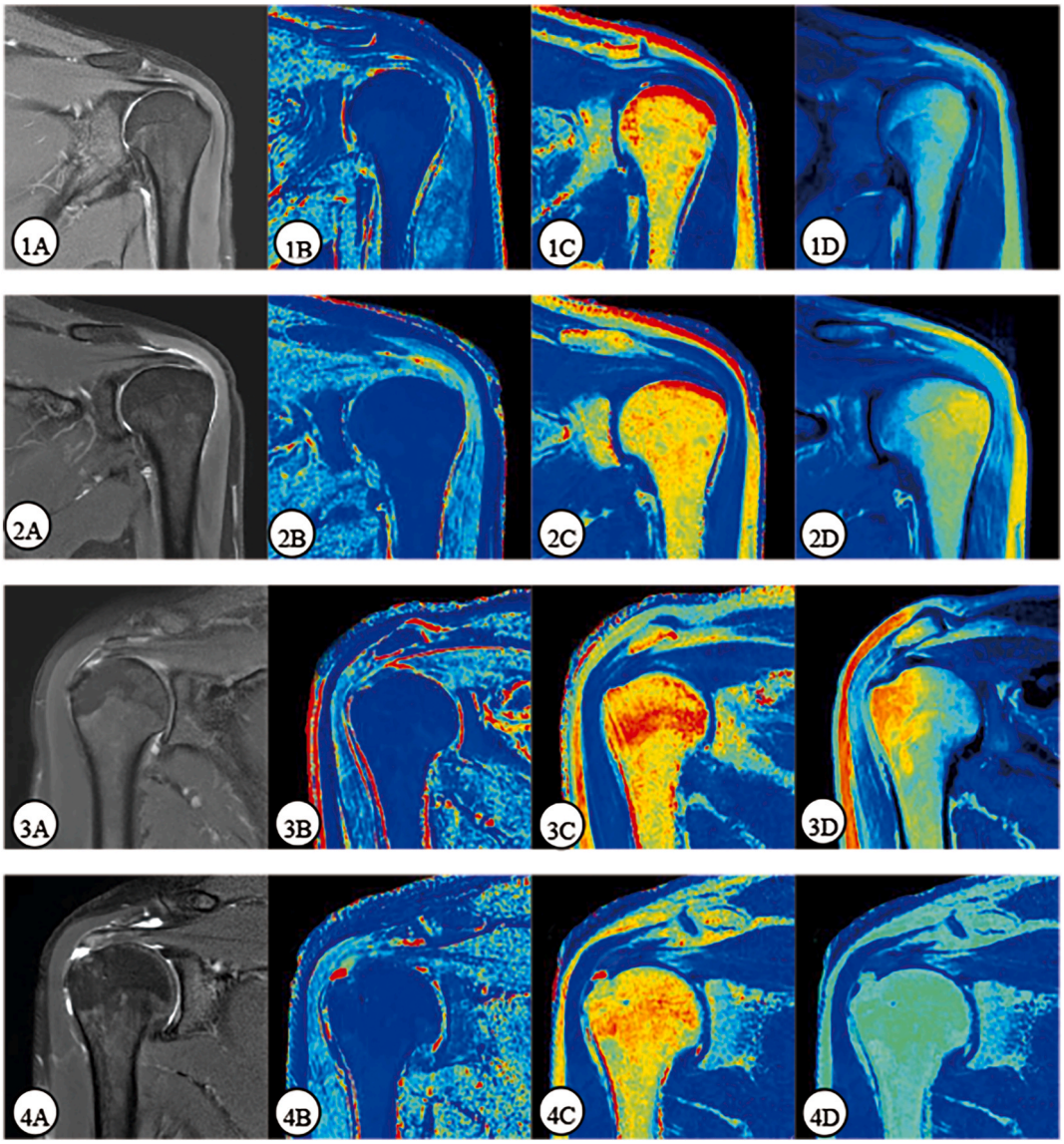

Fig. 5. Magnetic resonance imaging (MRI) images of different grades of RCI. (A–D) Grayscale images (A), T1-weighted (T1W) mapping (B), T2-weighted (T2W) mapping (C), and PD mapping (D) images of grade I, II, III, and IV RCI.

various grades of RCI with high AUCs. In addition, they showed a positive correlation with injury severity. This strong diagnostic capability stems from the close association of T2 values with tissue water content and collagen alignment [46], making them a biomarker for early soft tissue degeneration [47]. Notably, the central tendon region contains more water than the lateral region. When tendon pathology extends from the hypovascular zone near the humerus attachment, it triggers histopathological changes that are not readily visible in imaging but lead to increased T2 relaxation times. It suggests that RCI-related tissue changes affect the torn site and the intact tendon [48]. Elevated T2 values in the central subregion can indicate higher-grade injuries and a greater risk of future tearing, emphasizing the need for early intervention to improve the quality of life.

Muscle fat infiltration in the shoulder, particularly in RCI, is primarily linked to chronic pathological stimulation and the size and progression of the tear, often resulting in functional impairment of the shoulder joint and the deposition of fat within the shoulder muscles [32]. This study showed that the FF values in the supraspinatus, infraspinatus, and subscapularis muscles were significantly elevated in grade IV RCI, consistent with previous studies [49,50]. The increased fat in the supraspinatus and infraspinatus muscles in complete rotator cuff tears is due to nerve damage from muscle stress and the vulnerability of supraspinatus tendons to damage, leading to fibrous breakdown and fat replacement [51,52]. In the case of the subscapularis muscle, its sensitivity to hormones and metabolism also plays a role in fat accumulation. However, unlike the supraspinatus and infraspinatus muscles, the subscapularis muscle did not correlate positively with injury grading. It could be attributed to the subscapularis muscle's tendency to accumulate fat more prominently in severe and chronic RCI cases.

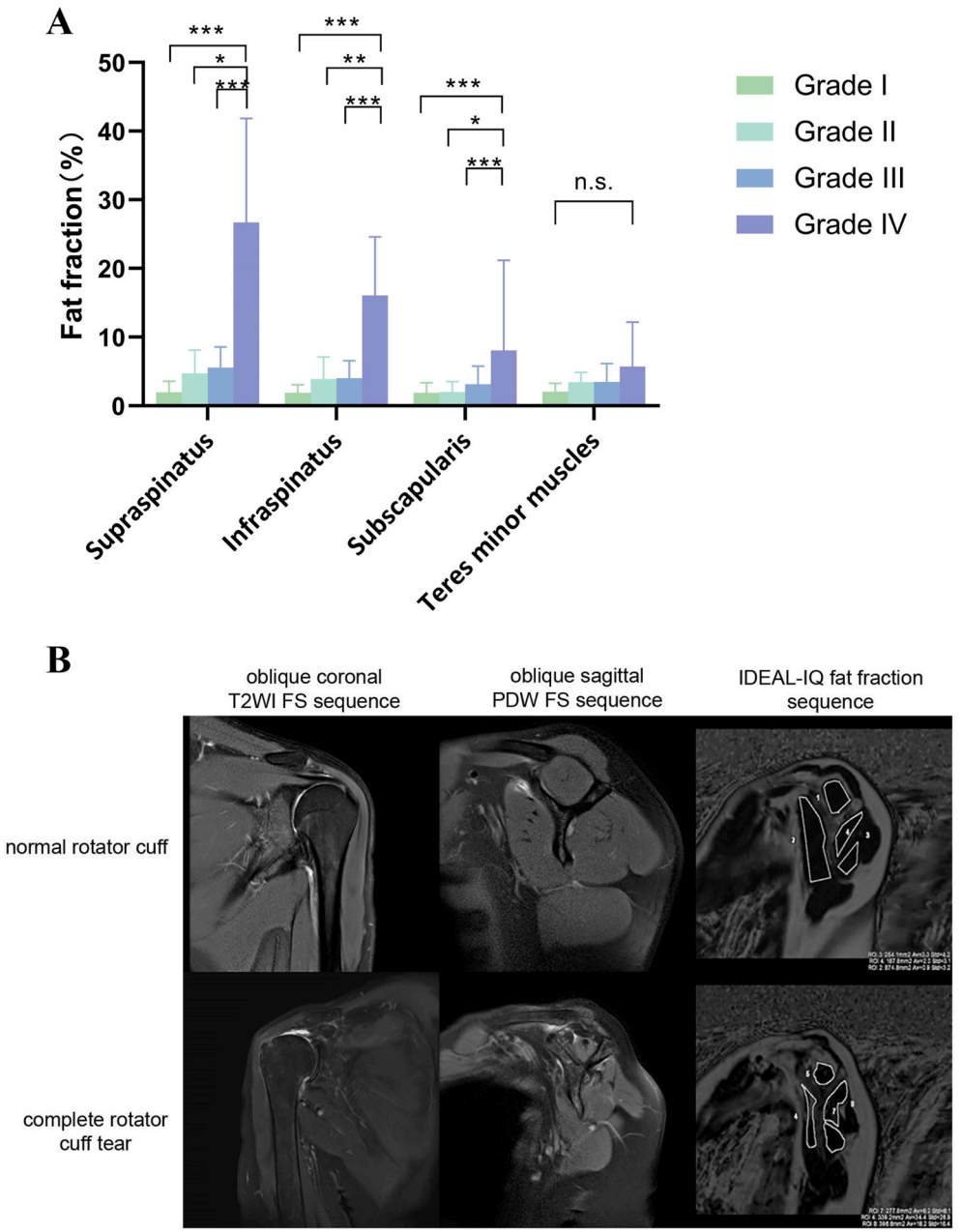

Fig. 6. Comparison of fat fraction (FF) values in rotator cuff muscles across different injury grades. (A) Bar graph showing FF values in the supraspinatus, infraspinatus, subscapularis, and teres minor muscles across different grades of RCI. Data are expressed as mean ± SD. *P < 0.05, **P < 0.01, ***P < 0.001, n.s, no statistically significant difference. (B) Magnetic resonance imaging (MRI) images of the shoulder joint comparing a normal rotator cuff (upper) to a complete rotator cuff tear (lower). From left to right: oblique coronal fat-saturated T2-weighted imaging (T2WI FS) sequence, oblique sagittal fat-saturated proton density-weighted (PDW) FS sequence, and iterative decomposition of water and fat with echo asymmetry and least squares estimation (IDEAL-IQ) fat fraction sequence.

In this study, the FF values of the four shoulder muscles did not significantly correlate with the VAS scores, likely because the main cause of pain in RCI is chronic inflammation [53] rather than a direct relationship with muscle fat infiltration, which is a secondary pathological change occurring in the later stages of the injury. On the other hand, FF values did exhibit a positive correlation with symptom duration. This correlation can be attributed to nerve damage in the muscles innervated by the suprascapular nerve, muscle atrophy, and increased fat infiltration caused by tendon rupture. These factors collectively lead to shoulder weakness and pain [54].

Several limitations of this study must be underlined. Firstly, the relatively small sample size, especially in the complete tear group, raises concerns about the statistical robustness and generalizability of the findings. The study included only 97 participants,

representing only a small proportion of the patients with RCI. The results should be confirmed in multicenter prospective studies. Secondly, the absence of clinical correlations, such as age, sex, and body mass index, which are known factors influencing RCI, diminishes the broader applicability of the results. This study did not correlate the imaging and the treatment approaches. Thirdly, while the study highlights the importance of MRI image quality, it failed to conduct a detailed evaluation of image quality or address possible artifacts that could affect measurement accuracy. Furthermore, the lack of external validation in diverse patient populations or clinical settings undermines the reliability and generalizability of the findings.

In conclusion, this study used advanced MRI techniques, including MRI integration sequence and IDEAL-IQ fat quantification, to assess and quantify RCI objectively. T2 values display a potential to differentiate between RCI grades, with a positive correlation with injury grading. The FF values in specific shoulder muscles also showed a promising potential to serve as reliable indicators of RCI severity. These results will have to be confirmed in larger trials.

Funding

This study was supported by the Key Research and Development Project of Ningxia Hui Autonomous Region, No. (2021BEG03033, 2023BEG03003)

Data availability

All data generated or analyzed during this study are included in this published article and its supplementary information files.

Ethical review committee statement

Therefore, it has been performed in accordance with the ethical standards laid down in the 1964 Declaration of Helsinki (Revised in 2013). This study was approved by the Medical Research Ethics Review Committee, General Hospital of Ningxia Medical University (KYLL-2022-1270). All patients provided written informed consent prior to treatment. All methods were carried out in accordance with relevant guidelines and regulations.

CRediT authorship contribution statement

Zhaorong Tian: Writing – review & editing, Writing – original draft, Validation, Methodology, Formal analysis. **Yabo Ni:** Writing – review & editing, Writing – original draft, Visualization, Resources, Data curation. **Hua He:** Writing – review & editing, Writing – original draft, Resources, Investigation, Data curation. **Bo Tian:** Writing – review & editing, Writing – original draft, Supervision, Methodology, Formal analysis. **Rui Gong:** Writing – review & editing, Writing – original draft, Resources, Project administration, Formal analysis. **Fenling Xu:** Writing – review & editing, Writing – original draft, Validation, Methodology, Formal analysis. **Zhijun Wang:** Writing – review & editing, Writing – original draft, Visualization, Project administration, Formal analysis.

Declaration of competing interest

The authors declare that they have no known competing financial interests or personal relationships that could have appeared to influence the work reported in this paper.

Appendix A. Supplementary data

Supplementary data to this article can be found online at https://doi.org/10.1016/j.heliyon.2024.e37307.

References

[1] A. Abdelwahab, N. Ahuja, K.P. Iyengar, V.K. Jain, N. Bakti, B. Singh, Traumatic rotator cuff tears - current concepts in diagnosis and management, Journal of clinical orthopaedics and trauma 18 (2021) 51–55.
[2] M. Adriani, M.F. Saccomanno, M. Motta, S. Galli, G. Milano, Reliability of magnetic resonance imaging criteria for the preoperative assessment of rotator cuff tears: a systematic review, Am. J. Sports Med. (2023) 3635465231166077.
[3] R.G. Ahmad, Shoulder impingement: various risk factors for supraspinatus tendon tear: a case group study, Medicine 101 (2022) e28575.
[4] E. Alipour, M. Chalian, A. Pooyan, A. Azhideh, F. Shomal Zadeh, H. Jahanian, Automatic MRI-based rotator cuff muscle segmentation using U-Nets, Skeletal Radiol. 53 (2024) 537–545.
[5] A.W. Anz, E.P. Lucas, E.K. Fitzcharles, R.K. Surowiec, P.J. Millett, C.P. Ho, MRI T2 mapping of the asymptomatic supraspinatus tendon by age and imaging plane using clinically relevant subregions, Eur. J. Radiol. 83 (2014) 801–805.
[6] A. Ashir, Y. Ma, S. Jerban, et al., Rotator cuff tendon assessment in symptomatic and control groups using quantitative MRI, J. Magn. Reson. Imag. : JMRI 52 (2020) 864–872.
[7] W. Bakhsh, G. Nicandri, Anatomy and physical examination of the shoulder, Sports Med. Arthrosc. Rev. 26 (2018) e10–e22.
[8] R.S. Boorman, K.D. More, R.M. Hollinshead, et al., What happens to patients when we do not repair their cuff tears? Five-year rotator cuff quality-of-life index outcomes following nonoperative treatment of patients with full-thickness rotator cuff tears, J. Shoulder Elbow Surg. 27 (2018) 444–448.

[9] D.L. Davis, R. Almardawi, R.F. Henn 3rd, et al., Correlation of quantitative versus semiquantitative measures of supraspinatus intramuscular fatty infiltration to shoulder range of motion and strength: a pilot study, Curr. Probl. Diagn. Radiol. 50 (2021) 629–636.
[10] D.L. Davis, M.N. Gilotra, J.P. Hovis, R. Almardawi, S.A. Hasan, Association of rotator cuff tear patterns and intramuscular fatty infiltration on magnetic resonance imaging, Journal of clinical imaging science 9 (2019) 38.
[11] S. Dogra, D.W. Dunstan, T. Sugiyama, A. Stathi, P.A. Gardiner, N. Owen, Active aging and public health: evidence, implications, and opportunities, Annu. Rev. Publ. Health 43 (2022) 439–459.
[12] J. Du, A.J. Chiang, C.B. Chung, et al., Orientational analysis of the Achilles tendon and enthesis using an ultrashort echo time spectroscopic imaging sequence, Magn. Reson. Imag. 28 (2010) 178–184.
[13] M. Etancelin-Jamet, L. Bouilleau, A. Martin, P. Bertrand, Diagnostic value of angled oblique sagittal images of the supraspinatus tendon for the detection of rotator cuff tears on MR imaging, Diagnostic and interventional imaging 98 (2017) 161–169.
[14] E. Ganal, C.P. Ho, K.J. Wilson, et al., Quantitative MRI characterization of arthroscopically verified supraspinatus pathology: comparison of tendon tears, tendinosis and asymptomatic supraspinatus tendons with T2 mapping, Knee Surg. Sports Traumatol. Arthrosc. : official journal of the ESSKA 24 (2016) 2216–2224.
[15] T. Hilbert, P. Omoumi, M. Raudner, T. Kober, Synthetic contrasts in musculoskeletal MRI: a review, Invest. Radiol. 58 (2023) 111–119.
[16] F.B. Hu, Y. Liu, W.C. Willett, Preventing chronic diseases by promoting healthy diet and lifestyle: public policy implications for China, Obes. Rev. : an official journal of the International Association for the Study of Obesity 12 (2011) 552–559.
[17] K.P. Hwang, S. Fujita, Synthetic MR: physical principles, clinical implementation, and new developments, Medical physics 49 (2022) 4861–4874.
[18] L. Zhang, W. Mai, X. Mo, et al., Quantitative evaluation of meniscus injury using synthetic magnetic resonance imaging, BMC Musculoskelet Disord 25 (2024) 292.
[19] Y. Jung, S.M. Gho, S.N. Back, T. Ha, D.K. Kang, T.H. Kim, The feasibility of synthetic MRI in breast cancer patients: comparison of T(2) relaxation time with multiecho spin echo T(2) mapping method, The British journal of radiology 92 (2019) 20180479.
[20] S. Eskreis-Winkler, G. Corrias, S. Monti, et al., IDEAL-IQ in an oncologic population: meeting the challenge of concomitant liver fat and liver iron, Cancer Imag. 18 (2018) 51.
[21] G. Zheng, F. Wei, P. Lu, et al., IDEAL-IQ measurement can distinguish dysplastic nodule from early hepatocellular carcinoma: a case-control study, Quant Imaging Med Surg 14 (2024) 3901–3913.
[22] M. Obrzut, V. Atamaniuk, K.J. Glaser, et al., Value of liver iron concentration in healthy volunteers assessed by MRI, Sci. Rep. 10 (2020) 17887.
[23] Y. Tian, P.F. Liu, J.Y. Li, Y.N. Li, P. Sun, Hepatic MR imaging using IDEAL-IQ sequence: will Gd-EOB-DTPA interfere with reproductivity of fat fraction quantification? World J Clin Cases 11 (2023) 5887–5896.
[24] R. Kijowski, J.M. Farber, J. Medina, W. Morrison, J. Ying, K. Buckwalter, Comparison of fat-suppressed T2-weighted fast spin-echo sequence and modified STIR sequence in the evaluation of the rotator cuff tendon, AJR. American journal of roentgenology 185 (2005) 371–378.
[25] J.K. Kloth, M. Winterstein, M. Akbar, et al., Comparison of 3D turbo spin-echo SPACE sequences with conventional 2D MRI sequences to assess the shoulder joint, Eur. J. Radiol. 83 (2014) 1843–1849.
[26] Y. Li, Y. Xiong, B. Hou, et al., Detection of erosions and fat metaplasia of the sacroiliac joints in patients with suspected sacroiliitis using a chemical shift-encoded sequence (IDEAL-IQ), Eur. J. Radiol. 158 (2023) 110641.
[27] Q. Ning, T. Fan, J. Tang, et al., Preliminary analysis of interaction of the fat fraction in the sacroiliac joint among sex, age, and body mass index in a normal Chinese population, J. Int. Med. Res. 48 (2020) 300060520931281.
[28] K.J. Jeon, C. Lee, Y.J. Choi, S.S. Han, Assessment of bone marrow fat fractions in the mandibular condyle head using the iterative decomposition of water and fat with echo asymmetry and least-squares estimation (IDEAL-IQ) method, PLoS One 16 (2021) e0246596.
[29] K.J. Jeon, Y.J. Choi, C. Lee, H.S. Kim, S.S. Han, Evaluation of masticatory muscles in temporomandibular joint disorder patients using quantitative MRI fat fraction analysis-Could it be a biomarker? PLoS One 19 (2024) e0296769.
[30] B.Y. Kong, S.H. Kim, D.H. Kim, H.Y. Joung, Y.H. Jang, J.H. Oh, Suprascapular neuropathy in massive rotator cuff tears with severe fatty degeneration in the infraspinatus muscle, The bone & joint journal 98-b (2016) 1505–1509.
[31] S. Lee, R.M. Lucas, D.A. Lansdown, et al., Magnetic resonance rotator cuff fat fraction and its relationship with tendon tear severity and subject characteristics, J. Shoulder Elbow Surg. 24 (2015) 1442–1451.
[32] T. Li, K. Mou, Y. Xiong, et al., Analysis of disease spectrum in outpatient department of shoulder joint sports injury, Chinese electronic journal of shoulder and elbow surgery 9 (2021) 148.
[33] D.J. Lin, M. Schwier, B. Geiger, et al., Deep learning diagnosis and classification of rotator cuff tears on shoulder MRI, Invest. Radiol. 58 (2023) 405–412.
[34] H.X. Liu, X.X. Xu, D.L. Xu, et al., The acromion-greater tuberosity impingement index: a new radiographic measurement and its association with rotator cuff pathology, J. Orthop. Surg. 28 (2020) 2309499020913348.
[35] Q. Ma, X. Cheng, X. Hou, Z. Yang, D. Ma, Z. Wang, Bone marrow fat measured by a chemical shift-encoded sequence (IDEAL-IQ) in patients with and without metabolic syndrome, J. Magn. Reson. Imag. : JMRI 54 (2021) 146–153.
[36] T.T. Ho, G.T. Kim, T. Kim, S. Choi, E.K. Park, Classification of rotator cuff tears in ultrasound images using deep learning models, Med. Biol. Eng. Comput. 60 (2022) 1269–1278.
[37] G. Ilyas, O. Gokalp, Reliability of ellman classification system in partial thickness rotator cuff tears on magnetic resonance views, Acta Chir. Orthop. Traumatol. Cech. 90 (2023) 259–266.
[38] L. Niglis, P. Collin, J.C. Dosch, N. Meyer, J.F. Kempf, SoFcot, Intra- and inter-observer agreement in MRI assessment of rotator cuff healing using the Sugaya classification 10years after surgery, Orthop Traumatol Surg Res 103 (2017) 835–839.
[39] H. Wu, Z. Zuo, Y. Li, et al., Anatomic characteristics of shoulder based on MRI accurately predict incomplete rotator cuff injuries in patients: relevance for predictive, preventive, and personalized healthcare strategies, EPMA J. 14 (2023) 553–570.
[40] T.R. Ahn, Y.C. Yoon, J.C. Yoo, H.S. Kim, J.H. Lee, Diagnostic performance of conventional magnetic resonance imaging for detection and grading of subscapularis tendon tear according to Yoo and Rhee classification system in patients underwent arthroscopic rotator cuff surgery, Skeletal Radiol. 51 (2022) 659–668.
[41] H.S. Mahon, J.E. Christensen, S.F. Brockmeier, Shoulder rotator cuff pathology: common problems and solutions, Clin. Sports Med. 37 (2018) 179–196.
[42] N. Matsumura, S. Oguro, S. Okuda, et al., Quantitative assessment of fatty infiltration and muscle volume of the rotator cuff muscles using 3-dimensional 2-point Dixon magnetic resonance imaging, J. Shoulder Elbow Surg. 26 (2017) e309–e318.
[43] R.M. Miller, J. Thunes, S. Maiti, V. Musahl, R.E. Debski, Effects of tendon degeneration on predictions of supraspinatus tear propagation, Ann. Biomed. Eng. 47 (2019) 154–161.
[44] A.L. Minkalis, R.D. Vining, C.R. Long, C. Hawk, K. de Luca, A systematic review of thrust manipulation for non-surgical shoulder conditions, Chiropr. Man. Ther. 25 (2017) 1.
[45] S.J. Nho, H. Yadav, M.K. Shindle, J.D. Macgillivray, Rotator cuff degeneration: etiology and pathogenesis, Am. J. Sports Med. 36 (2008) 987–993.
[46] C.P.L. Paul, T.H. Smit, M. de Graaf, et al., Quantitative MRI in early intervertebral disc degeneration: T1rho correlates better than T2 and ADC with biomechanics, histology and matrix content, PLoS One 13 (2018) e0191442.
[47] A. Shams, M. El-Sayed, O. Gamal, W. Ewes, Subacromial injection of autologous platelet-rich plasma versus corticosteroid for the treatment of symptomatic partial rotator cuff tears, European journal of orthopaedic surgery & traumatology : Orthop. Traumatol. 26 (2016) 837–842.
[48] H. Tang, F. Luo, H. Fan, et al., Acupuncture and manual therapy for rotator cuff tears: a protocol for systematic review and meta analysis, Medicine 99 (2020) e20377.
[49] R.Z. Tashjian, J. Shin, K. Broschinsky, et al., Minimal clinically important differences in the American Shoulder and Elbow Surgeons, Simple Shoulder Test, and visual analog scale pain scores after arthroscopic rotator cuff repair, J. Shoulder Elbow Surg. 29 (2020) 1406–1411.

[50] W.J. Tu, X. Zeng, Q. Liu, Aging tsunami coming: the main finding from China's seventh national population census, Aging clinical and experimental research 34 (2022) 1159–1163.
[51] C. Wang, Q. Hu, W. Song, W. Yu, Y. He, Adipose stem cell-derived exosomes decrease fatty infiltration and enhance rotator cuff healing in a rabbit model of chronic tears, Am. J. Sports Med. 48 (2020) 1456–1464.
[52] Z. Zeng, X. Ma, Y. Guo, B. Ye, M. Xu, W. Wang, Quantifying bone marrow fat fraction and iron by MRI for distinguishing aplastic anemia from myelodysplastic syndromes, J. Magn. Reson. Imag. : JMRI 54 (2021) 1754–1760.
[53] T. Zhou, C. Han, X. Weng, Present situation and development prospects of the diagnosis and treatment of rotator cuff tears, Frontiers in surgery 10 (2023) 857821.
[54] M.B. Zlatkin, J.P. Iannotti, M.C. Roberts, et al., Rotator cuff tears: diagnostic performance of MR imaging, Radiology 172 (1989) 223–229.